3D Channel Model for MIMO Polarized Antennas

[#]Dao Manh Tuan [1], Seong-Ook Park[2]
[1] Electrical Engineering Department, Korean Advanced Institute of Science and Technology
7117-N27-KAIST, tuandm@kaist.ac.kr
[2] Electrical Engineering Department, Korean Advanced Institute of Science and Technology
7105-N27-KAIST, sopark@ee.kaist.ac.kr

Abstract

We propose a three-dimensional (3D) polarized MIMO channel model, which takes into account 3D power angular spectrum and comprehensive propagation characteristics of electromagnetic waves excited by polarized antennas. Based on the model, we derive a close form expression of the spatial correlation as a function of the physical parameters representing both characteristics of arbitrary antennas and propagation environment in 3D space. The spatial correlation expression allows to use the Von Mises Fisher (VMF) distribution, resulting in a more accurate and general channel model. Through simulation, we evaluate and compare performance, in terms of the spatial correlation and capacity, of 2×2 MIMO antenna configurations with different polarizations, i.e. V/V, V/H, and slanted $\pm 45^0$ polarizations. The effect of the parameters is analyzed, and verified in certain cases through the literature.

Keywords : Antennas, MIMO, polarization, XPD, 3D, polarized channels, correlation, capacity.

1. Introduction

MIMO systems are considered a potential solution to the demand for high data rates. The major issue of MIMO systems is that capacity gain is highly dependent on the spatial correlation, which is a function of the antenna array and channel characteristics [1]. It has been shown that, in order to achieve reasonably low correlation, antenna spacing has to be at least half a wavelength, resulting in increasing equipment size. The use of cross-polarized antenna has an advantage to reduce the spacing required on terminal. Thus, this approach is receiving considerable attention in the design of MIMO antennas. Implementation and evaluation of MIMO systems need a comprehensive understanding of MIMO channels. Despite a number of channel models for polarized antennas, the limitation of these works is that the propagating waves are assumed to arrive only from the azimuth plane therefore not include the elevation spectrum, thus not fully considering the characteristics of antenna and environmental factors.

In this paper, we propose a 3D polarized geometry model that can accurately represent important aspects of polarized MIMO channels in 3D space. We derive the close-form expression of the spatial correlation as a function of the physical parameters representing both characteristics of arbitrary antennas and propagation environment in 3D space. The close-form expression allows to integrate the Von Mises Fisher (VMF) distribution, which has been proved to be appropriate for modeling spherical data [2] to the model, resulting in a more accurate and general channel model. Using this model, we investigate the effect of elevation angle and antenna orientation, on performance of a 2×2 MIMO systems with different polarizations of antennas.

2. Channel Modeling

Consider a MIMO system with S transmit antennas (Tx_1,...,Tx_S) and U receive antennas (Rx_1,...,Rx_U) under a 3D geometry model, as shown in Fig. 1. The model is a two-sphere 3D geometrical model, which can be considered as an extension of the two-ring model [3]. It is assumed that energy contribution of remote scatterers is negligible, only local scatterers at both ends of radio link are considered. The transmitter is fixed and the receiver is in motion with the velocity vector **v**. There are K and L scatterers at the transmitter and receiver, respectively. The K scatterers are assumed to lie on a spherical surface of radius R_T and the kth transmit scatterer, denoted as TS_k

($k = 1, 2, \ldots, K$), is specified by the solid angle $\Omega_k^{Tx}(\varphi_k,\ \vartheta_k)$ which follows a given angular distribution. Similarly, the L scatterers are assumed to lie on a spherical surface of radius R_R and the lth receive scatterer, denoted as RS_l ($l = 1, 2, \ldots, L$), is specified by the solid angle $\Omega_l^{Rx}(\phi_l,\ \theta_l)$ which follows a given angular distribution. The symbols φ_k and ϑ_k denote the azimuth angle of departure (AAoD) and elevation angle of departure (EAoD), respectively. Similarly, the symbols ϕ_l and θ_l denote the azimuth angle of arrival (AAoA) and elevation angle of arrival (EAoA), respectively. The distance between the centers of the transmitter and receiver is D. For the local scattering assumption, the radii R_T and R_R are much smaller than the distance D ($R_{T,}\ R_R \ll D$). The antenna configuration at both transmitter and receiver is assumed to be uniform linear array (ULA). The spacing between antenna elements at the transmitter and receiver is denoted by d_T and d_R, respectively. The orientation of antenna array at the transmitter (Tx) and receiver (Rx) are specified by the angles φ_{Tx} , ϑ_{Tx} , ϕ_{Rx} and θ_{Rx}.

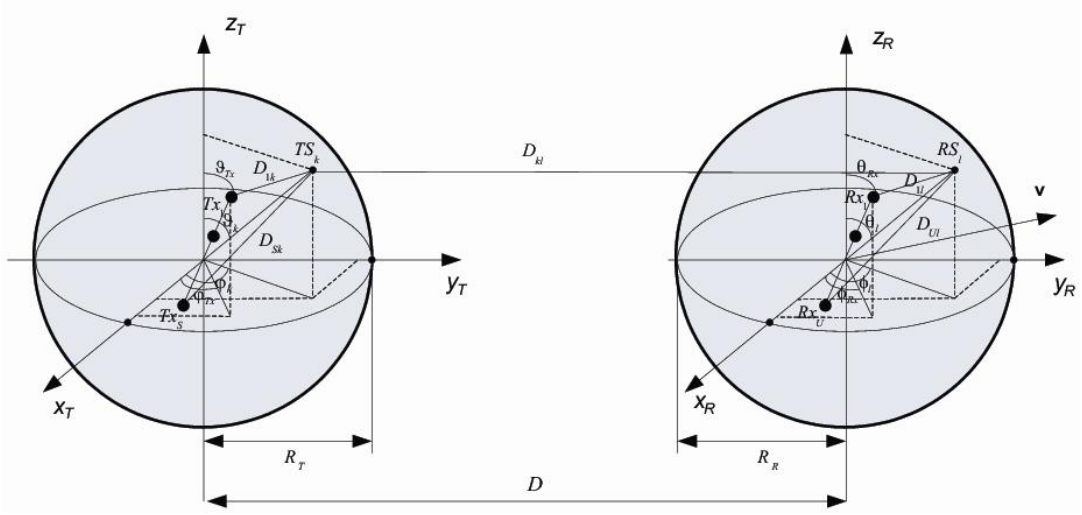

Figure 1: Illustration of 3D channel model.

It is assumed that the system is under non-line-of-sight (NLOS) and flat fading environment, the (u, s)component ($u = 1, 2, \ldots, U; s = 1, 2, \ldots, S$) of channel matrix $\mathbf{H}(t)$, can be written as

$$h_{u,s}(t) = \sqrt{P_{us}} \lim_{K,L\to\infty} \frac{1}{\sqrt{KL}} \sum_{k=1}^{K} \sum_{l=1}^{L} g_{l,k} \times \exp\left(-jk_0(D_{sk} + D_{kl} + D_{lu})\right) \exp(j\mathbf{k_l}\mathbf{v})t$$
$$\times \begin{bmatrix} F_s^{Tx(v)}(\Omega_k^{Tx}) \\ F_s^{Tx(h)}(\Omega_k^{Tx}) \end{bmatrix}^T \begin{bmatrix} \exp(j\Phi_{l,k}^{(v,v)}) & \sqrt{\kappa_{l,k}^h}\sqrt{\chi_{l,k}}\exp(j\Phi_{l,k}^{(v,h)}) \\ \sqrt{\kappa_{l,k}^v}\exp(j\Phi_{l,k}^{(h,v)}) & \sqrt{\chi_{l,k}}\exp(j\Phi_{l,k}^{(h,h)}) \end{bmatrix} \begin{bmatrix} F_u^{Rx(v)}(\Omega_l^{Rx}) \\ F_u^{Rx(h)}(\Omega_l^{Rx}) \end{bmatrix} \quad (1)$$

where P_{us} is the power transfered through the subchannel $Tx_s - Rx_u$; $g_{l,k}$ and $\Phi_{l,k}^{(x,y)}$ are the gain and phase shift between V (H) component of the transmit antenna and V (H) component of the receive antenna, respectively, caused by the interaction of the local scatterers TS_k and RS_l; D_{sk} is the distance from the scatterer TS_k to the sth transmit antenna Tx_s; D_{lu} is the distance from the scatterer RS_l to the uth receive antenna Rx_u; D_{lk} is the distance from the scatterer TS_k to the scatterer RS_l; $F_s^{Tx(v)}(\Omega_k^{Tx})$ and $F_s^{Tx(h)}(\Omega_k^{Tx})$ are the complex field patterns of the sth transmit antenna Tx_s for V polarization and H polarization respectively; $F_u^{Rx(v)}(\Omega_l^{Rx})$ and $F_u^{Rx(h)}(\Omega_l^{Rx})$ the complex field pattern of the uth receive antenna Rx_u for V polarization and H polarization respecively; $\kappa_{k,l}^v$and $\kappa_{k,l}^h$ are the inverse XPD for VV/HV and HH/VH transmission, respectively; $\chi_{l,k}$ is the inverse of the co-polar ratio (CPR); k_0 is the wavenumber, $k_0 = 2\pi/\lambda$ where λ is the wavelength; $\mathbf{k_l}$ denotes the wave vector pointing in the propagation direction from the scatterer RS_l and $j = \sqrt{-1}$. By the central limit theorem, with the given statistical properties of the channel, as K and L, the numbers of scatterers at the Tx and Rx, approach infinity, the $h_{u,s}(t)$ approaches a circularly symmetric Gaussian random process with mean zero and variance $E\left[\left|h_{u,s}(t)\right|^2\right]$.

Therefore, the channel becomes a purely Rayleigh-fading process. The channel coefficient $h_{u,s}(t)$ is unnormalized. If the channel coefficient is normalized as $h_{u,s}^{norm}(t) = h_{u,s}(t) / \sqrt{E\left[\left|h_{u,s}(t)\right|^2\right]}$, the normalized channel coefficient $h_{u,s}^{norm}(t)$ has the standard normal distribution, $\widetilde{N}(0, 1)$. Consequently, the channel matrix is properly modeled as matrix **H** with the normalized channel coefficient $h_{u,s}^{norm}(t)$. If we define $\mathrm{vec}(\mathbf{H}) = (\mathbf{H}_1^T, \mathbf{H}_2^T, \ldots, \mathbf{H}_S^T)^T$, where $\mathbf{H}_i (i = 1, \ldots, S)$ is the $U \times 1$ matrix and $[\cdot]^T$ denotes transposition, we can determine the spatial correlation matrix of the vec (**H**) as follows:

$$\mathbf{R} \triangleq \mathrm{cov}(\mathrm{vec}(\mathbf{H})) = E\left[\mathrm{vec}(\mathbf{H})\mathrm{vec}^{\mathrm{H}}(\mathbf{H})\right]. \tag{2}$$

Since the vec(**H**) constructed from the model is special complex Gaussian, the second-order statistics of the vec(**H**) are completely specified by the cov(vec(**H**)) [4]. The spatial correlation between $h_{p,m}^{norm}(t)$ and $h_{q,n}^{norm}(t)$, denoted as $r_{pm,qn}(t)$, is written as

$$r_{pm,qn}(t) = E[h_{p,m}^{norm}(t)h_{q,n}^{norm*}(t)] = \frac{E[h_{p,m}(t)h_{q,n}^*(t)]}{\sqrt{E\left[|h_{p,m}(t)|^2\right]}\sqrt{E\left[|h_{q,n}(t)|^2\right]}}. \tag{3}$$

After mathematical transformations (not shown due to the limit of paper), the correlation in (3) is eventually

$$\begin{aligned}
&E[h_{p,m}(t)h_{q,n}^*(t)] = \sqrt{P_{pm}P_{qn}} \\
&\times \Big(\int_0^{2\pi}\int_0^{\pi} \exp\left(-j(a\sin\vartheta\cos\varphi + b\sin\vartheta\sin\varphi + c\cos\vartheta)\right) F_m^{Tx(v)}(\varphi,\vartheta)F_n^{Tx(v)}(\varphi,\vartheta)p^{Tx}(\varphi,\vartheta)\sin\vartheta d\vartheta d\varphi \\
&\times \int_0^{2\pi}\int_0^{\pi} \exp\left(-j(d\sin\theta\cos\phi + f\sin\theta\sin\phi + g\cos\theta)\right) F_p^{Rx(v)}(\phi,\theta)F_q^{Rx(v)}(\phi,\theta)p^{Rx}(\phi,\theta)\sin\theta d\theta d\phi \\
&+ E[1/Y_1]\int_0^{2\pi}\int_0^{\pi} \exp\left(-j(a\sin\vartheta\cos\varphi + b\sin\vartheta\sin\varphi + c\cos\vartheta)\right) F_m^{Tx(h)}(\varphi,\vartheta)F_n^{Tx(h)}(\varphi,\vartheta)p^{Tx}(\varphi,\vartheta)\sin\vartheta d\vartheta d\varphi \\
&\times \int_0^{2\pi}\int_0^{\pi} \exp\left(-j(d\sin\theta\cos\phi + f\sin\theta\sin\phi + g\cos\theta)\right) F_p^{Rx(v)}(\phi,\theta)F_q^{Rx(v)}(\phi,\theta)p^{Rx}(\phi,\theta)\sin\theta d\theta d\phi \\
&+ E[1/Y_2]E[1/Y_3]\int_0^{2\pi}\int_0^{\pi} \exp\left(-j(a\sin\vartheta\cos\varphi + b\sin\vartheta\sin\varphi + c\cos\vartheta)\right) F_m^{Tx(v)}(\varphi,\vartheta)F_n^{Tx(v)}(\varphi,\vartheta)p^{Tx}(\varphi,\vartheta)\sin\vartheta d\vartheta d\varphi \\
&\times \int_0^{2\pi}\int_0^{\pi} \exp\left(-j(d\sin\theta\cos\phi + f\sin\theta\sin\phi + g\cos\theta)\right) F_p^{Rx(h)}(\phi,\theta)F_q^{Rx(h)}(\phi,\theta)p^{Rx}(\phi,\theta)\sin\theta d\theta d\phi \\
&+ E[1/Y_3]\int_0^{2\pi}\int_0^{\pi} \exp\left(-j(a\sin\vartheta\cos\varphi + b\sin\vartheta\sin\varphi + c\cos\vartheta)\right) F_m^{Tx(h)}(\varphi,\vartheta)F_n^{Tx(h)}(\varphi,\vartheta)p^{Tx}(\varphi,\vartheta)\sin\vartheta d\vartheta d\varphi \\
&\times \int_0^{2\pi}\int_0^{\pi} \exp\left(-j(d\sin\theta\cos\phi + f\sin\theta\sin\phi + g\cos\theta)\right) F_p^{Rx(h)}(\phi,\theta)F_q^{Rx(h)}(\phi,\theta)p^{Rx}(\phi,\theta)\sin\theta d\theta d\phi\Big)
\end{aligned} \tag{4}$$

where

$a = k_0(m-n)d_T sin\vartheta_{Tx} cos\varphi_{Rx}$; $b = k_0(m-n)d_T sin\vartheta_{Tx} sin\varphi_{Rx}$; $c = k_0(m-n)d_T cos\vartheta_{Tx}$;
$d = k_0(p-q)d_R sin\theta_{Tx} cos\phi_{Rx}$; $f = k_0(p-q)d_R sin\theta_{Tx} sin\phi_{Rx}$; $g = k_0(p-q)d_R cos\theta_{Tx}$;
$Y_1 = \mathrm{XPD}_v$; $Y_2 = \mathrm{XPD}_h$; $Y_3 = \mathrm{CPR}$. The terms $p^{Tx}(\varphi,\vartheta)$ and $p^{Rx}(\phi,\theta)$, the scatterer distributions at the transmitter and receiver, are modeled as Von Mises Fisher (VMF) distributions [2]

$$p^{Tx(Rx)} = \sum_{i=1}^{N_{Tx(Rx)}} \nu_i^{Tx(Rx)} f(\Omega^{Tx(Rx)}|\Omega_i^{Tx(Rx)}, \zeta_i^{Tx(Rx)})$$

where N_{Tx} and N_{Rx} are the number of clusters at the transmitter and receiver; $\nu_i^{Tx(Rx)}$ is defined as the prior probability that the *i*th cluster was generated; $\Omega_i^{Tx(Rx)}$ and $\zeta_i^{Tx(Rx)}$ are the mean direction and concentration of the *i*th cluster, respectively.

It is observed that, the XPD and CPR, when expressed in decibel (dB), have the normal distribution, $\widetilde{N}(\mu,\sigma)$. Depending on the environment, the mean μ of XPD varies from 0 to 18 dB, with the standard deviation σ in order of 3-8 dB [5]. The mean of CPR varies between 0 and 6 dB [6]. The expectations in (4) are computed by [7]

$$E[1/Y] = \int_0^{\infty} \frac{1}{\sqrt{2\pi\sigma^2}} \frac{10}{y^2 \ln 10} \exp\left(-\frac{(\frac{10\ln y}{\ln 10} - \mu)^2}{2\sigma^2}\right) dy = \exp\left(\frac{\sigma^2 \ln^2 10}{200} - \frac{\mu \ln 10}{10}\right). \tag{5}$$

From the spatial correlation matrix, $\mathbf{R} = \mathrm{cov}\big(\mathrm{vec}(\mathbf{H})\big) = \mathbf{R}^{1/2}(\mathbf{R}^{1/2})^{\mathrm{H}}$, whose entries are computed by (3), we can generate samples of channel matrix as follows:

$$\mathbf{H} = \mathrm{unvec}(\mathbf{R}^{1/2}\mathrm{vec}(\mathbf{H}_{\mathrm{w}})) \tag{6}$$

where $\mathbf{H_w}$ is matrix with complex Gaussian elements. Because the samples of the channel maintain the spatial correlation of **H**, we can say that its spatial characteristics are the same as those of the real channel.

3. Simulation and Discussion

This section evaluates performance of MIMO transmission in terms of capacity and correlation of a 2×2 MIMO system with different polarization antenna configurations, as shown in Fig. 2. It is assumed that in the system described by (1) the transmitter has no channel-state information, and only the receiver knows the actual realizations. This implies that the signals are independent and the power is equally divided among the transmit antennas. Under this assumption, the capacity of MIMO channel is given by

$$C = \log_2 \left[\det(\mathbf{I} + \frac{\rho}{S}\mathbf{H}\mathbf{H}^T) \right] \tag{7}$$

where ρ is the average signal-to-noise ratio (SNR), **I** is the identity matrix, and **H** is the normalized channel matrix, which is computed by (6). Dual-polarized configurations suffer from subchannel power losses, which need to be accounted for in their capacity calculation. If we use a fixed transmit power constraint, we normalize the channel so as to achieve an average of ρ_0 (ρ_0 is chosen as 10 dB in this simulation) on the vertical-to-vertical link. As a result, the SNR is equal to ρ [6]

$$\rho = \rho_0 \frac{1}{1 + E[1/\mathrm{XPD}]}. \tag{8}$$

The angular profiles vary depending on the physical layout of the propagation environment. Extraction of the VMF parameters requires measurement campaign and data processing. For purpose of simulation, we use the result of the VMF parameters for the AoA profile in [2], as shown in Fig. 3. It is noticed from Fig. 3 that the main energy of incoming waves comes from the direction $(\phi, \theta) = (330^0, 90^0)$.

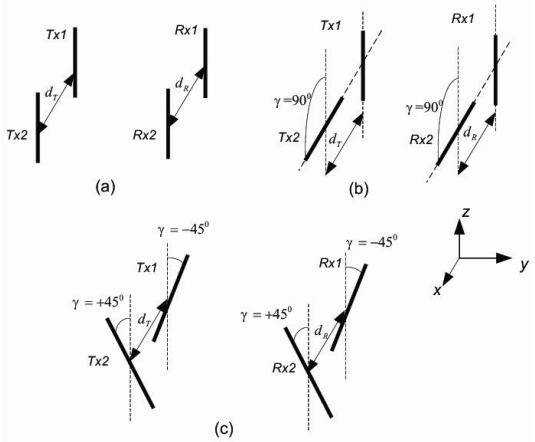

Figure 2: Configurations of antennas for different polarizations. (a) Vertical polarization. (b) V/H polarization. (c) Slanted $\pm 45^0$ polarization

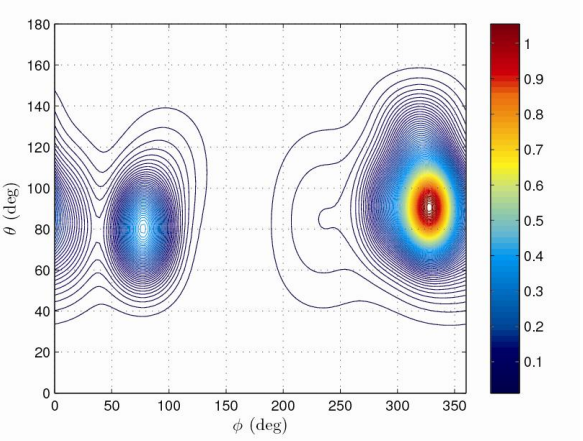

Figure 3: Contour plot of AOA

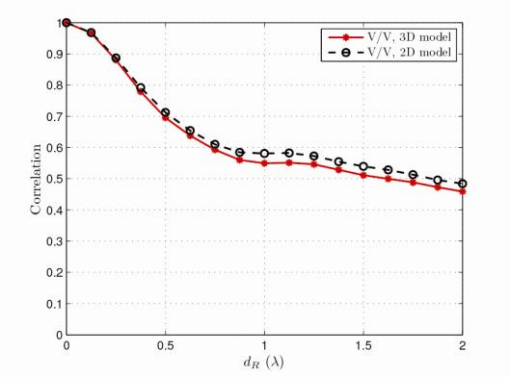

(a)

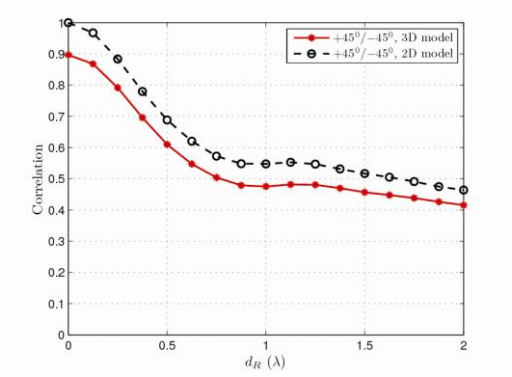

(b)

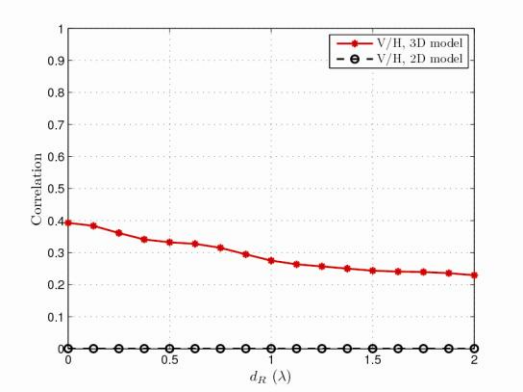

(c)

Figure 4. Performance comparison between 3D model and 2D model (a) Vertical polarization. (b) $\pm 45^0$polarization. (c) V/H polarization.

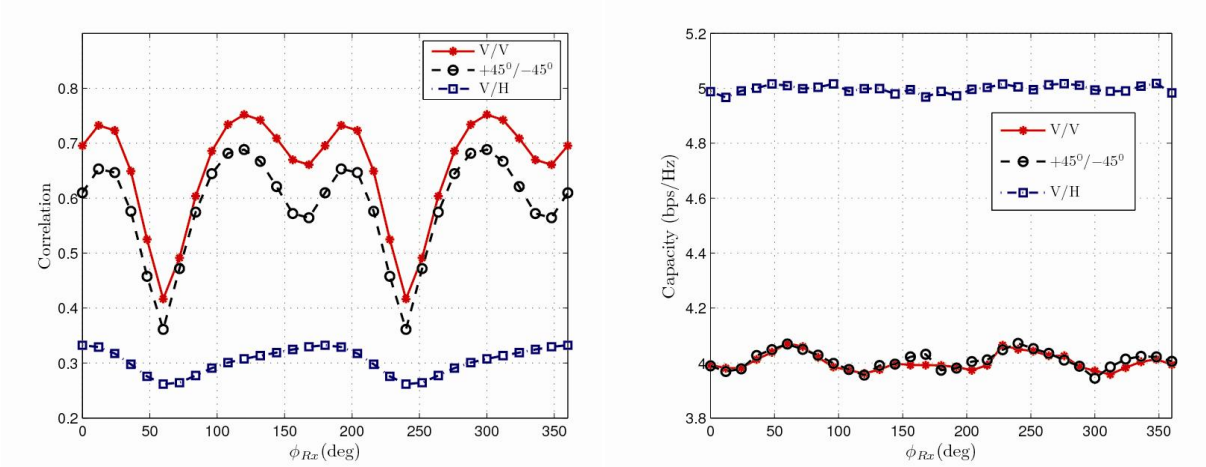

Figure 5. Performance versus antenna orientation: (a) Correlation. (b) Capacity.

We study the effect of elevation angle by evaluating MIMO performance of the configurations under the 3D model and under the 2D model that is transformed from the 3D model by setting the elevation angles $\vartheta = \theta = \pi/2$ integrating the integrand in (4) over the azimuth domain only. It is observed in Fig. 4 that the 2D channel model gives higher correlation for the configurations with the V/V and slanted $\pm 45^0$ polarizations (Fig. 4 (a) and (b)). However, it is interesting to note that the 2D channel model provides the correlation of zero for the configuration with the V/H polarization (Fig. 4 (c)). This is because the 2D model considers antenna pattern in azimuth plane only. The vertical components of the dipole with inclination angle of 90^0 is only equal to zero in the plane $\theta = \pi/2$. In this case, omission of the vertical components of the 2D model makes the orthogonality of polarization between the two antennas at the transmitter and receiver, yielding zero correlation. Therefore, depending on the configurations, the 2D model would underestimate or overestimate MIMO performance. On the other hand, the influence of patterns among elements is important to the study on the effect of elevation angle. In [8], the assumption of identical dipoles for all elements only results in the underestimation of the capacity that is not true in general.

The effect of antenna orientation on the correlation is shown in Fig. 5. The correlation varies as a function of ϕ_{Rx} and gets minimum when ϕ_{Rx} is approximately equal to 60^0 or to 240^0. This is because, at these values, the main direction of incoming waves, which is shown in Fig. 3, is perpendicular to the receive array. Intuitively, since the distance between the two sub-channels $Tx_1 - Rx_1$ and $Tx_2 - Rx_2$ is maximum, the correlation is minimum. It also found in Fig. 5 (a) that the correlation of the configuration with the V/H polarization is the lowest among the configurations, and that the correlation of the configuration with the slanted $\pm 45^0$ polarization is lower than that of the configuration with the V/V polarization. Similar experimental observation can be found in [9]. The behavior of the correlation results in that of the average capacity as shown Fig. 5 (b). It is indeed found that the capacity is the highest at 60^0 or at 240^0 In addition, although the

correlation of the configuration with the V/V polarization is higher than that of the slanted $\pm 45^0$ polarization, their capacity is almost the same, varying between 3.9 and 4.1 bps/Hz. This is because the configuration employing the slanted $\pm 45^0$ polarization suffers from the power loss as a consequence of the amount of depolarization. It is also found that the capacity of the configuration with the V/H polarization is almost constant at 5 bps/Hz, or 20% higher than that of the configurations with the V/V and slanted $\pm 45^0$ polarizations. Thus, the V/H polarization is effective from the viewpoint of the correlation to enhance the capacity in MIMO channels.

5. Conclusion

This paper proposes a 3D polarized channel model for MIMO systems. In this model, the scatterers are distributed over the sphere centered on the antenna array. The probability distribution of scatterers is based on the VMF distribution that is suitable for directions in space. In particular, derivation of a close form expression for the spatial correlation matrix which completely characterizes the spatial properties of the channel has been presented. Comparison in terms of the correlation between the 2D and 3D channel models has been made to show the inaccurate estimation of the 2D model in the scenarios. The proposed model can be used to evaluate the effect of arbitrary parameters on performance of MIMO systems in terms of both correlation and capacity. The proposed model is presented here for linear array, but can be extended to any kind of array type.

References

[1] D. Gesbert, M. Shafi, D. shan Shiu, P. Smith, and A. Naguib, "From theory to practice: An overview of MIMO space-time coded wireless systems," IEEE J. Sel. Areas Commun., vol. 21, no. 3, pp. 281–302 Apr. 2003.

[2] Mammasis, R. Stewart, and J. Thompson, "Spatial fading correlation model using mixtures of Von Mises Fisher distributions," IEEE Trans. Wireless Commun., vol. 8, no. 4, pp. 2046 – 2055, Apr. 2009.

[3] G. Byers and F. Takawira, "Spatially and temporally correlated MIMO channels: Modeling and capacity analysis," IEEE Trans. Veh. Technol., vol. 53, no. 3, pp. 634 – 643, May 2004.

[4] E. I. Telatar and D. Tse, "Capacity of and muatual information of broad- band multipath fading channels," in Proc. IEEE Int. Symp. Information Theory, 1998, p. 188.

[5] M. Shafi, M. Zhang, A. Moustakas, P. Smith, A. Molisch, F. Tufvesson, and S. Simon, "Polarized MIMO channels in 3-D: models, measurements and mutual information," IEEE J. Sel. Areas Commun., vol. 24, no. 3, pp. 514–527, Mar. 2006.

[6] C. Oestges, B. Clerckx, M. Guillaud, and M. Debbah, "Dual-polarized wireless communications: From propagation models to system performance evaluation," IEEE Trans. Wireless Commun., vol. 7, no. 10, pp. 4019–4031, Oct. 2008.

[7] M. T. Dao, V. A. Nguyen, and S. O. Park, "Derivation and analysis of spatial correlation for 2×2 MIMO system," IEEE Antennas Wireless Propag. Lett., vol. 8, pp. 409–413, 2009.

[8] M. Shafi, M. Zhang, P. Smith, A. Moustakas, and A. Molisch, "The impact of elevation angle on MIMO capacity," in Proc. ICC 2006 - IEEE Int. Conf. Communications, vol. 9, Jun. 2006, pp. 4155–4160.

[9] K. Nishimori, Y. Makise, M. Ida, R. Kudo, and K. Tsunekawa, "Channel capacity measurement of 8 × 2 MIMO transmission by antenna configurations in an actual cellular environment," IEEE Trans. Antennas Propag., vol. 54, no. 11, pp. 3285–3291, Nov. 2006.